Brief Report

Changes of arachnoid granulations after subarachnoid hemorrhage in cynomolgus monkeys

Yuanpei Jiang[1], Lei Meng[2], Jinxiang Yan[3], Hongsheng Yue[1], Jie Zhu[1], Yuguang Liu[4,*]

[1] Department of Neurosurgery, Jinan Central Hospital, Cheeloo College of Medicine, Shandong University, 250013 Jinan, Shandong, China

[2] Department of Neurosurgery, Shandong Provincial Hospital, Cheeloo College of Medicine, Shandong University, 250021 Jinan, Shandong, China

[3] Department of Neurosurgery, The First People's Hospital of Tai'an Ningyang County, 271400 Tai'an, Shandong, China

[4] Department of Neurosurgery, Qilu Hospital, Cheeloo College of Medicine, Shandong University, 250021 Jinan, Shandong, China

*Correspondence: yuguangliu2012@gmail.com (Yuguang Liu)

DOI:10.31083/j.jin2002043

Submitted: 13 December 2020 Revised: 12 January 2021 Accepted: 28 April 2021 Published: 30 June 2021

This research explores ultrastructural changes of arachnoid granulations associated with hydrocephalus after subarachnoid hemorrhage in cynomolgus monkeys. It provides a theoretical basis for further study of the etiology and prevention of hydrocephalus. Female cynomolgus monkeys about one-year-old were selected. The position range of arachnoid granulations in superior sagittal sinus and transverse sinus was determined in a randomly selected control monkey. The morphology of normal arachnoid granulations in cynomolgus monkeys was observed under a transmission electron microscope. A primate model of subarachnoid hemorrhage was established by injecting autologous blood into cisterna magna. Vomiting, movement disorder, and reduced level of consciousness were gradually observed in monkeys. Computed tomography and magnetic resonance imaging scan results confirmed subarachnoid hemorrhage and hydrocephalus, and the morphology of arachnoid granulations in hydrocephalus was observed under a transmission electron microscope. Extensive fibrosis of arachnoid granulations was observed under a transmission electron microscope in cynomolgus monkeys with hydrocephalus after subarachnoid hemorrhage.

Keywords

Subarachnoid hemorrhage; Arachnoid granulations; Hydrocephalus; Fibrosis; Nonhuman primates

1. Introduction

Hydrocephalus is a common complication after aneurysm subarachnoid hemorrhage (SAH) [1]. According to the classical bulk flow theory, cerebrospinal fluid (CSF) flows through the fourth ventricle outlets into the subarachnoid space around the brain and the spinal cord before it is finally reabsorbed the venous system through arachnoid granulations (AGs) in the sagittal sinus. The blockage of AGs by red blood cells and their decomposition products causes CSF absorption disorder and ultimately results in chronic hydrocephalus [2]. However, there is still no definite quantitative experiment to confirm CSF absorption by AGs. In addition, some researchers believe that CSF flows into the extracranial lymphatic system through lymphatic vessels associated with the extracranial segments of cranial nerves [3]. Research on the circulation pathways of CSF has mainly been conducted on rats and dogs, which is unable to fully explain human CSF circulation. As AGs differ hugely in different species and different developmental stages, we believe that the reabsorption pathways of CSF are diverse and of different significances. We speculate that animals with a developed sense of smell mainly rely on the powerful extracranial lymphatic system to absorb CSF, while primates mainly rely on AGs. Previous researchers have used various experimental animals to study the CSF circulation pathways, but differences in species have led to different experimental results [4]. Based on our experimental conditions, preliminary research, and pertinent literature, we selected cynomolgus monkeys as experimental subjects, which are more similar to humans in anatomy, hoping to draw more accurate conclusions. In this research, we established hydrocephalus primate models after SAH by repeatedly injecting autologous blood into the subarachnoid space of cynomolgus monkeys to observe the ultrastructural changes of AGs under pathological conditions, in hopes of providing a theoretical basis for the etiology and prevention of hydrocephalus after SAH.

2. Materials and methods

2.1 Primate model preparation

Female cynomolgus monkeys about one year old weighing 3.1 to 4.0 kilograms were selected as experimental subjects. Each monkey was labeled randomly, with its weight, age, sex, height, and other data recorded. Three monkeys were randomly selected as control (labeled as C1, C2, and C3), and head CT and MRI scans were performed on them. After anesthetized with intravenous injection of xerazine hydrochloride (0.1–0.2 mg/kg), C1, C2 and C3 were decapitated, and then their upper sagittal sinus and transverse sinus were taken out, embedded in paraffin, and sliced. The location of AGs was determined by Hematoxylin and Eosin (HE) staining. Then tissues of AGs were removed and put under a transmission electron microscope to have their morphology observed.

Journal of Integrative Neuroscience

The monkeys in the experimental group were randomly labeled as M2, M3, M4, M5, M6, and M7, respectively. They were anesthetized by intravenous injection of xerazine hydrochloride. After fixed in a prone position, disinfected, and skin-prepared, each monkey was injected with 2–3 mL of autologous blood from the femoral vein of the lower limbs into the subarachnoid space through the cisterna magna (an equivalent amount of CSF was replaced). The above operations were repeated on the 5th, 9th, and 13th days to establish SAH primate models. During the next four days, head CT and brain MRI were performed on the monkeys with vomiting, movement disorder, and reduced level of consciousness. Those monkeys showing subarachnoid hemorrhage and obstructive hydrocephalus were considered to be successful primate models. The experiment was conducted in Shandong Hongli Medical Animal Experimental Research Co., Ltd., under the supervision of the Animal Ethics Committee of Shandong Hongli Medical Animal Experimental Research Co., Ltd. All operations in this experiment complied with "Regulations on the Administration of Laboratory Animals" of the People's Republic of China.

2.2 Imaging

CT: After anesthesia, the cynomolgus monkey was lying supinely on the CT diagnostic bed, with its abdomen mid-sagittal plane perpendicular to the bed and aligned with the longitudinal midline of the bed. CT imaging was performed on a 256-slice Helical CT scanner (Brilliance iCT; Philips Healthcare; parameters: 128×0.625 collimation, 0.601 pitch, 120 kV, 300 mAs, 0.5 s rotation time, 2.8 s scan time). Images were reconstructed by a hybrid iterative reconstruction technique (iDose4; Philips Healthcare).

MR: After the cynomolgus monkey was anesthetized, its upper jaw and both external auditory canals were fixed, and a Philips 3.0T superconducting MR imaging system and a matching head orthogonal unique coil were used for head MR plain scan to obtain continuous imaging (scanning sequence: Spin echo T1WI (TR561 ms, TE17 ms), Fast Spin Echo T2WI (TR3900 ms, TE102 ms); layer thickness 5 mm, interval 5 mm, field of view 40×40 cm^2, matrix 320×320).

2.3 Hematoxylin and Eosin staining

The five monkeys with hydrocephalus were executed by decapitation under anesthesia 17 days after the first blood injection. Their skin was cut longitudinally along the midline of the head, and then their periosteum was peeled off. Their skulls were removed to expose both cerebral hemispheres, and then their dura mater was cut. Superior sagittal sinus and transverse sinus tissues were quickly removed, trimmed to 10 mm, and fixed directly with 4% paraformaldehyde. The fixed tissues were dehydrated with gradient alcohol (80%, 90%, 95%, 100%), non-opacified with xylene, immersed entirely in melted paraffin, moved into embedding frames filled with melted paraffin, cooled to solidification, sliced to 5-μm sections, and stained with HE.

2.4 Transmission electron microscope

Superior sagittal sinus and transverse sinus specimens of hydrocephalus monkeys were removed and trimmed to 1 mm^3 as quickly as possible, fixed with 2.5% glutaraldehyde fixative for two hours, and then washed three times with PBS (pH 7.4) buffer. Then the tissues were dehydrated with a gradient of acetone (70% acetone, 15 minutes; 80% acetone, 15 minutes; 90% acetone, 15 minutes; 100% acetone, 10 minutes). The tissues were embedded in embedding cassettes, which were then left to polymerize and harden in an oven at 45–60 °C to form embedded blocks and taken out after the oven cooled naturally to room temperature. After sliced into 10-μm sections and stained with uranyl acetate and lead citrate, the tissues were observed under transmission electron microscope. Three collagen fiber (CF) groups with the longest diameters in three randomly selected fields of view were measured, expressed as (mean $\pm$ SD).

3. Results

First of all, head CT examination results performed on normal cynomolgus monkeys showed that their bilateral cerebral hemispheres' size, shape, and location were normal, with no apparent abnormal density shadows in the brain parenchyma. The shape, size, and location of their ventricles were normal. Their brain cistern and sulci were not enlarged (Fig. 1A). Simultaneous brain MRI scans showed no abnormal signals (Fig. 1B,C). HE staining of normal cynomolgus monkey intracranial tissues showed that the normal arachnoid granular structure exists in the superior sagittal sinus. Its structure and position are similar to those of humans (Fig. 2A,B). The endothelial cells in the outermost layer of normal AGs and layered fibrocytes and connective tissue fibers, were observed under an electron microscope (Fig. 2C,D).

After confirming the location and structure of cynomolgus AGs, we began to prepare primate models of SAH. After receiving repeated autologous blood injections into the subarachnoid space through the cisterna magna, cynomolgus monkeys gradually showed signs of movement disorder (limb weakness and movement decrease), anorexia, and unresponsiveness. The weights of the monkeys were lowered to 2.78 to 3.63 kilograms. Then head CT scan showed high-density shadows in the subarachnoid space (Fig. 3C), and both head CT and MR (Fig. 3D) showed dilation of the ventricular system. The imaging results above suggested the formation of hydrocephalus after SAH. Hydrocephalus monkeys were dissected, and the subarachnoid space was congested with blood clots (Fig. 4). The arachnoid granular tissues of the monkeys with hydrocephalus were observed under a transmission electron microscope. The outer arachnoid was filled with red blood cells (Fig. 5A). Condensation and marginalization of some nucleus chromation were observed, part of the mitochondria and endoplasmic reticulum were swollen with vacuoles, apoptosis and necrosis were found in the endothelial cells of AGs, and the connective tissue scaffold around the

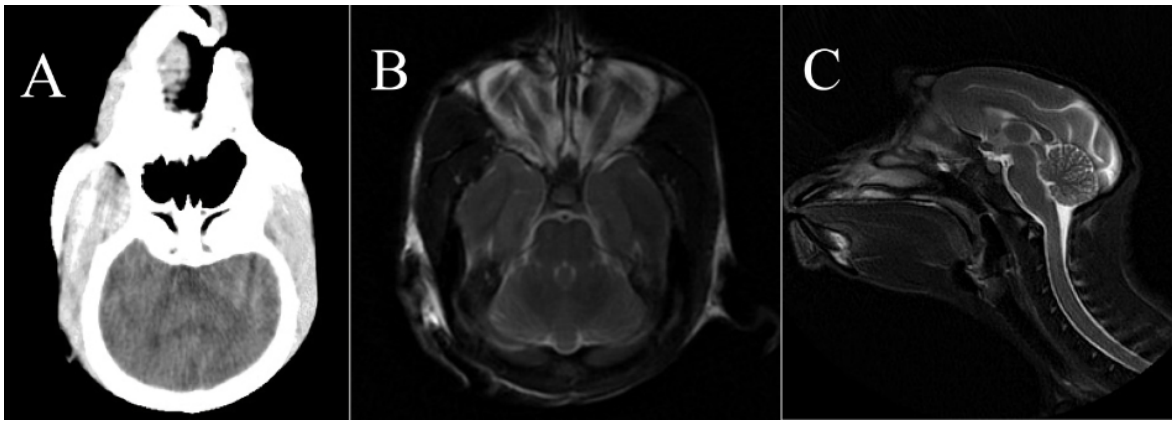

Fig. 1. Representative imaging of normal cynomolgus monkeys. (A) Head CT shows normal. No mass, hemorrhage, or hydrocephalus. Basal ganglia and posterior fossa structures are normal. No major established vessel vascular territory infarction. No intra- or extra-axial collection. The basal cisterns and foramen magnum are patents. (B,C) Brain MRI shows normal. No abnormal focal areas of altered signal intensity in the cerebral hemispheres, brainstem, or cerebellum. The appearance and intensity of brain parenchyma are normal. The ventricular system and cisternal spaces appear normal. No evidence of intracranial space occupying lesion or apparent vascular anomaly is detected. There is no shift of the midline structures.

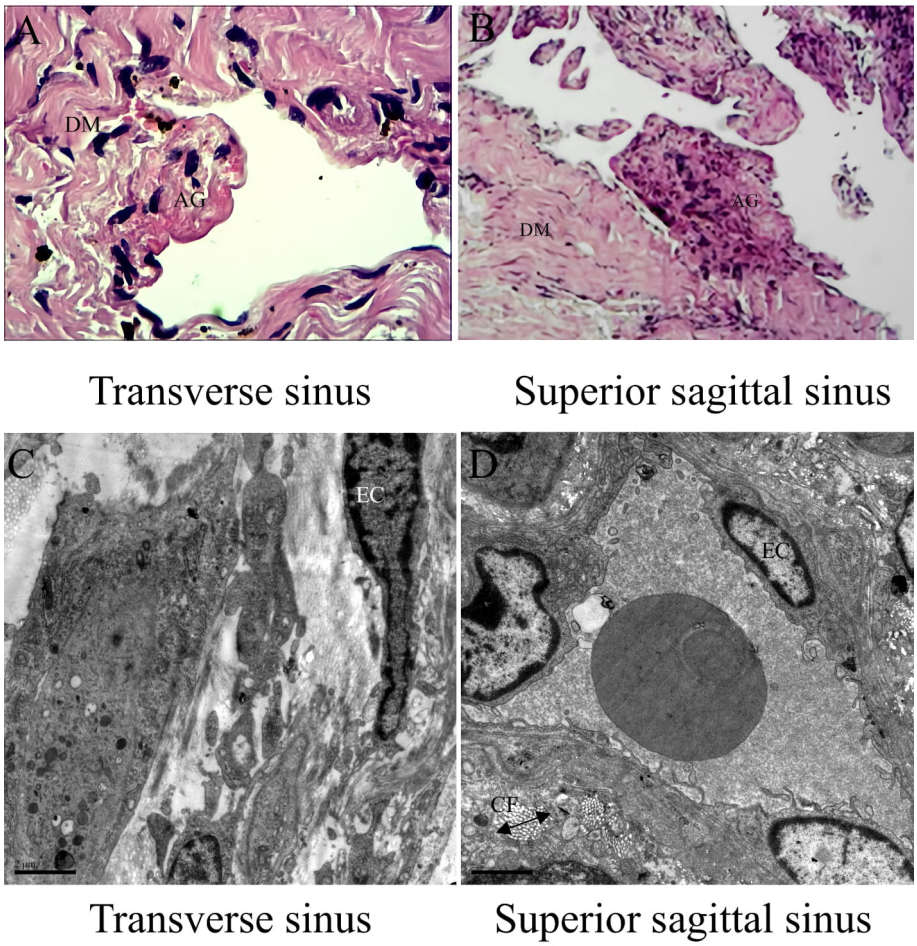

Fig. 2. Ultrastructure of normal AGs. (A,B) HE staining shows that AGs composed of endothelial cells protrude into the sinus lumen. The endothelial cells in the outermost layer of normal AGs and layered fibrocytes and connective tissue fibers, are present under a transmission electron microscope. (C) Endothelial cells and adjacent fibroblasts in the outermost layer of AGs from the transverse sinus of normal cynomolgus monkeys. (D) Endothelial cells and adjacent fibroblasts of AGs from the superior sagittal sinus of normal cynomolgus monkeys. DM, dura mater; AG, Arachnoid Granulation; CF, collagen fiber; EC, endothelial cell; Double arrow, the thickness of CF; (A,B) 40×; (C,D) Scale bar = 2 μm.

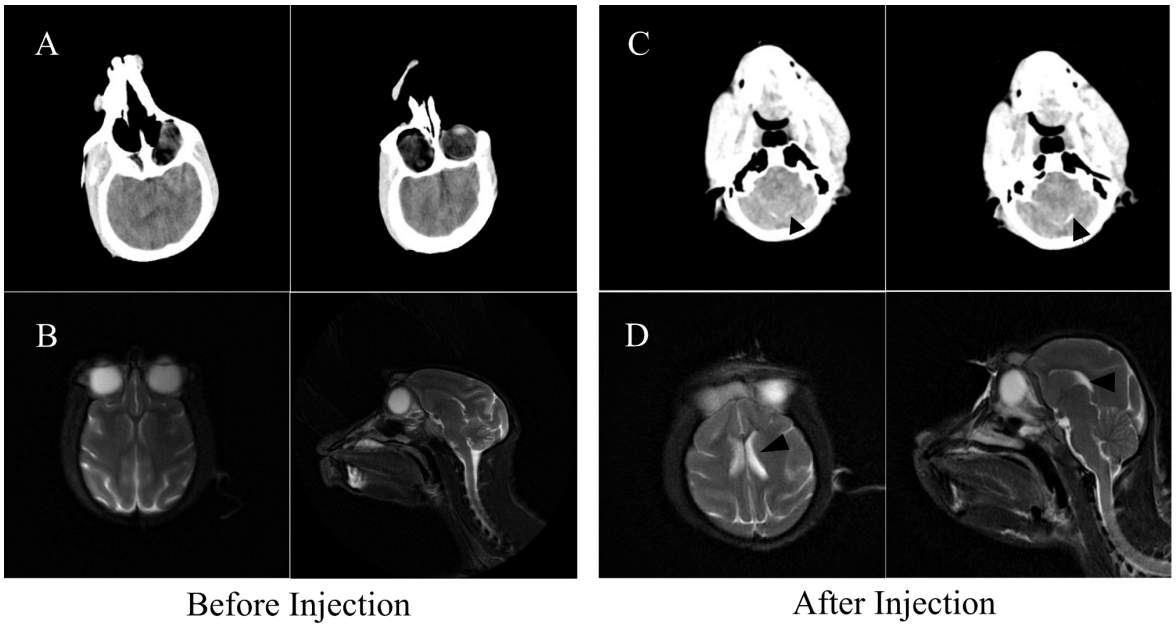

Fig. 3. Imaging of cynomolgus monkeys before and after blood injection. (A,B) Both head CT and Brain MRI show normal. (C) After injecting autologous blood through the occipital cistern, the head CT of cynomolgus monkeys shows high-density shadows in the subarachnoid space (black arrows). (D) After the injection, MRI of cynomolgus monkeys shows dilation of the ventricular system.

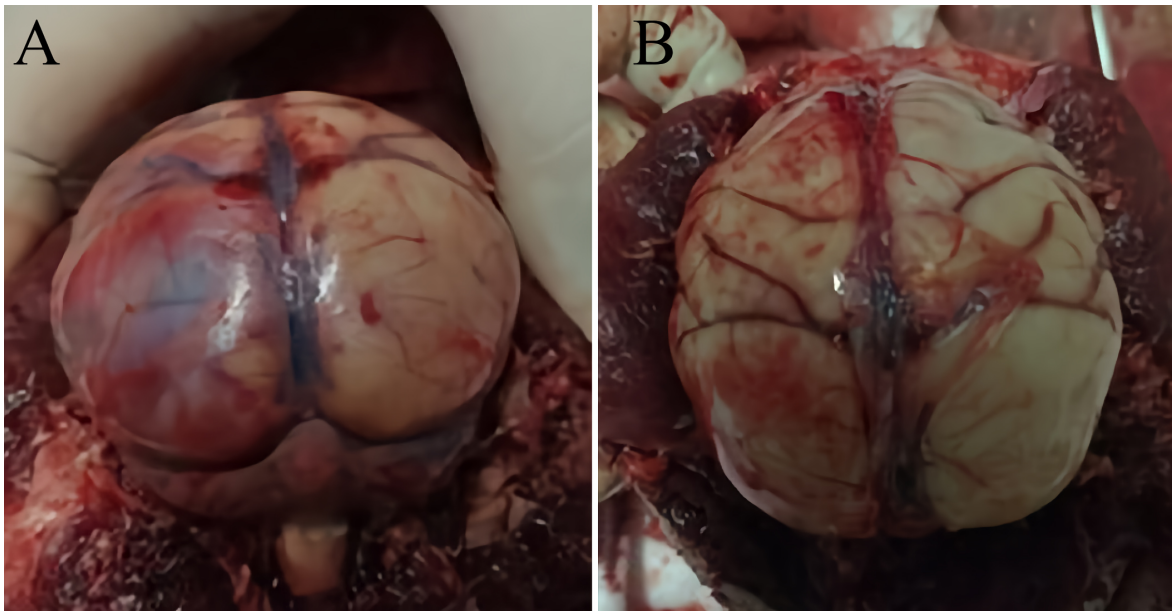

Fig. 4. Monkeys were dissected, and the subarachnoid space was congested with blood clots. (A) Blood clots under the dura. (B) Blood clots full of sulci and gyri.

cells was disordered and thickened. Collagen fiber hyperplasia was observed, and the fibrous connective tissue of the outer arachnoid layer was thicker than normal (Fig. 5B–D). For a more intuitive comparison, we measured the CF thicknesses of normal and pathological AGs. We found that CF in normal AGs (Fig. 5E,F) is scattered, and the thickest part measures 2 ± 0.54 μm, while in the AGs of monkeys suffering hydrocephalus after SAH, CF thickness is about 4 ± 1.23 μm. All these signs suggested that AGs suffered extensive fibrosis.

4. Discussion

AGs, also known as arachnoid villi and pacchionian granulations, are small protrusions of the arachnoid mater into the outer membrane of the dura mater. They protrude into the dural venous sinuses of the brain and allow CSF to pass from the subarachnoid space into the bloodstream. AGs were first discovered by the Italian scholar Antoine Pacchion in the

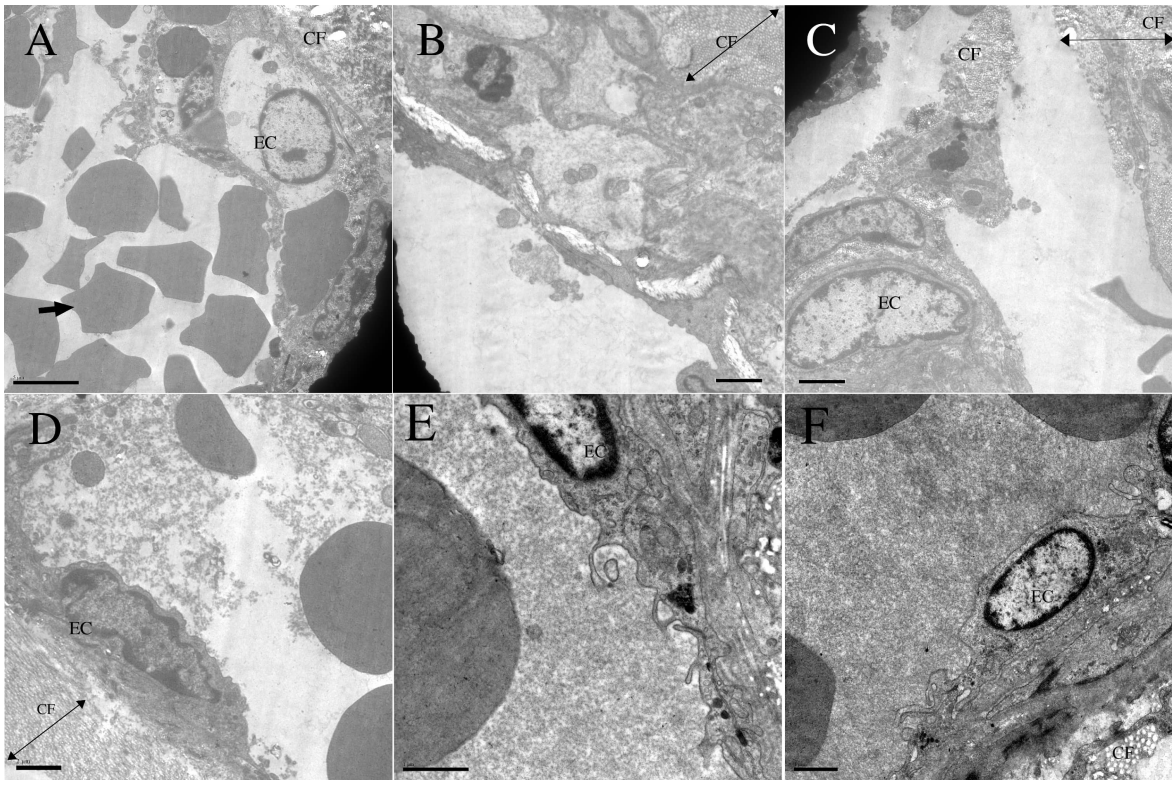

Fig. 5. Ultrastructure of AGs after SAH in cynomolgus monkeys. (A) The outer arachnoid is filled with red blood cells (indicated by a black arrow). (B–D) The fibrous connective tissue of the outer arachnoid layer appears thicker than normal, and AGs show extensive fibrosis. (E,F) CF in normal AGs is scattered. (A) Scale bar = 5 μm, (B–D) Scale bar = 2 μm, (E,F) Scale bar = 1 μm.

18th century [5]. Later studies confirmed that AGs have begun to form in the superior sagittal sinus, parasagittal sinus, and transverse sinus within one to two months before birth, which gradually develops under the permanent pressure of CSF after birth. Human AGs are mainly distributed in the superior sagittal sinus (53%), especially where the central vein joins the superior sagittal sinus; followed by the transverse sinus (28%), especially where the vein of Labbe merges into the transverse sinus; some in the straight sinuses (17%); and the rest in the intracranial venous sinuses [6, 7]. Conegero *et al.* [8] used scanning electron microscopy to find that human AGs are composed of pedicle, body, and apex, and are surrounded by a capsule of connective tissues composed of bundles of collagen fibers that form pores of different shapes and sizes. In addition, there are unique connections between arachnoid cells to facilitate the flow of CSF [8]. However, the role of AGs in CSF circulation is controversial. According to some research, most CSF flows out through lymphatic vessels associated with the extracranial segments of cranial nerves.

Acute obstructive hydrocephalus and chronic communicating hydrocephalus may occur after SAH. Obstructive hydrocephalus mainly occurs within three days after SAH and is caused by sudden obstruction of CSF circulation, accompanied by acute intracranial pressure increase and consciousness disorders. Communicating hydrocephalus mainly occurs two weeks after SAH, and it typically manifests itself as mental retardation, gait anomalies, and urinary incontinence. The pathogenesis of hydrocephalus after SAH has not been fully elucidated. Early researchers found that arachnoid cell proliferation caused by inflammation or blood coagulation products can block CSF flow through AGs into venous sinuses. With the emergence of a large number of studies on hydrocephalus after SAH since the 1970s [9, 10], more and more evidence supports that the inflammatory reaction and subsequent fibrotic process impede the outflow of CSF from AGs to sinuses. This research mainly focuses on the pathological obstruction of AGs, including mechanical obstruction and fibrosis of AGs. Previous studies have proposed that blood clots play an initial role in triggering the excessive secretion of CSF and fibrosis of arachnoid granulation, thereby causing long-term communicating hydrocephalus rather than mere aqueduct obstruction or stenosis [11]. With the emergence of abundant evidence of fibrotic pathways, it is generally believed that the fibrosis and adhesion of leptomeningeal and AGs cause chronic communicating hydrocephalus. Red blood cell metabolites, especially iron, have long been assumed to play important roles in the pathophysiological processes of chronic hydrocephalus after SAH. Previous studies suggested that iron oxidation accounts for the precise mechanisms of pathogenesis of hydrocephalus [12], initially termed "ferroptosis" [13]. Intraventricular injection of iron (ferrous chloride or ferric chloride) or lysed

red blood cells into rats will lead to hydrocephalus [14]. In addition, iron also causes necrosis of brain cells and disruption of the blood-brain barrier in rats [15], which adds to the strength of this hypothesis. In this research, cynomolgus monkeys were used as research subjects due to their similar anatomy to humans. Repeated injection of autologous blood into the cisterna magna led to hydrocephalus, and other results confirmed extensive fibrosis of AGs. Our results further confirmed the above theory, but more evidence is still needed to further clarify the connection between "ferroptosis" and hydrocephalus.

We look forward to a credible clinical trial to establish whether the removal of blood clots or subarachnoid blood lavage in the initial stage of SAH will produce positive results for these patients.

Regarding research limitations, the observed subjects were insufficient, which may cause biased results, so repeating the experiment with larger sample sizes is necessary. Furthermore, we only monitored the morphological changes of arachnoid particles. To prove the correlation between iron and the pathogenesis of hydrocephalus, quantitative research on iron and other inflammation-related factors in AGs should be conducted.

Author contributions

YL guaranteed the integrity of the entire study. LM designed the study. HY, JZ, and YJ performed the research. YJ analyzed the data. YJ, JY, and YL wrote the manuscript. All authors contributed to editorial changes in the manuscript. All authors read and approved the final manuscript.

Ethics approval and consent to participate

This experiment was conducted in Shandong Hongli Medical Animal Experimental Research Co., Ltd., under the supervision of the Animal Ethics Committee of Shandong Hongli Medical Animal Experimental Research Co., Ltd. All operations in this experiment complied with "Regulations on the Administration of Laboratory Animals" of the People's Republic of China.

Acknowledgment

We would like to thank all the reviewers for their opinions and suggestion.

Funding

This work was supported by Jinan outstanding talent fund sponsored project (2015).

Conflict of interest

The authors declare no conflict of interest.

References

[1] Xie Z, Hu X, Zan X, Lin S, Li H, You C. Predictors of Shunt-dependent Hydrocephalus after aneurysmal subarachnoid hemorrhage? A systematic review and meta-analysis. World Neurosurgery. 2017; 106: 844–860.e6.

[2] Chen S, Luo J, Reis C, Manaenko A, Zhang J. Hydrocephalus after subarachnoid hemorrhage: pathophysiology, diagnosis, and treatment. BioMed Research International. 2017; 2017: 8584753.

[3] Louveau A, Plog BA, Antila S, Alitalo K, Nedergaard M, Kipnis J. Understanding the functions and relationships of the glymphatic system and meningeal lymphatics. The Journal of Clinical Investigation. 2017; 127: 3210–3219.

[4] Shapey J, Toma A, Saeed SR. Physiology of cerebrospinal fluid circulation. Current Opinion in Otolaryngology & Head & Neck Surgery. 2019; 27: 326–333.

[5] Brunori A, Vagnozzi R, Giuffrè R. Antonio Pacchioni (1665–1726): early studies of the dura mater. Journal of Neurosurgery. 1993; 78: 515–518.

[6] Liang L, Korogi Y, Sugahara T, Ikushima I, Shigematsu Y, Takahashi M, *et al.* Normal structures in the intracranial dural sinuses: delineation with 3D contrast-enhanced magnetization prepared rapid acquisition gradient-echo imaging sequence. AJNR. American Journal of Neuroradiology. 2002; 23: 1739–1746.

[7] Gailloud P, Muster M, Khaw N, Martin JB, Murphy KJ, Fasel JH, *et al.* Anatomic relationship between arachnoid granulations in the transverse sinus and the termination of the vein of Labbe: an angiographic study. Neuroradiology. 2001; 43, 139–143.

[8] Conegero CI, Chopard RP. Tridimensional architecture of the collagen element in the arachnoid granulations in humans: a study on scanning electron microscopy. Arquivos De Neuro-Psiquiatria. 2003; 61: 561–565.

[9] Alksne JF, Lovings ET. The role of the arachnoid villus in the removal of red blood cells from the subarachnoid space. An electron microscope study in the dog. Journal of Neurosurgery. 1972; 36: 192–200.

[10] Massicotte EM, Del Bigio MR. Human arachnoid villi response to subarachnoid hemorrhage: possible relationship to chronic hydrocephalus. Journal of Neurosurgery. 1999; 91: 80–84.

[11] Kanat A, Turkmenoglu O, Aydin MD, Yolas C, Aydin N, Gursan N, *et al.* Toward changing of the pathophysiologic basis of acute hydrocephalus after subarachnoid hemorrhage: a preliminary experimental study. World Neurosurgery. 2013; 80: 390–395.

[12] Chen Q, Tang J, Tan L, Guo J, Tao Y, Li L, *et al.* Intracerebral hematoma contributes to hydrocephalus after intraventricular hemorrhage via aggravating iron accumulation. Stroke. 2015; 46: 2902–2908.

[13] Dixon SJ, Lemberg KM, Lamprecht MR, Skouta R, Zaitsev EM, Gleason CE, *et al.* Ferroptosis: an iron-dependent form of non-apoptotic cell death. Cell. 2012; 149: 1060–1072.

[14] Gao C, Du H, Hua Y, Keep RF, Strahle J, Xi G. Role of red blood cell lysis and iron in hydrocephalus after intraventricular hemorrhage. Journal of Cerebral Blood Flow and Metabolism. 2014; 34: 1070–1075.

[15] Chen Q, Zhang J, Guo J, Tang J, Tao Y, Li L, *et al.* Chronic hydrocephalus and perihematomal tissue injury developed in a rat model of intracerebral hemorrhage with ventricular extension. Translational Stroke Research. 2015; 6: 125–132.